

Efficient procedure for failure probability function estimation in augmented space

Xiukai Yuan^{a,c,*}, Shaolong Liu^a, M.A. Valdebenito^b, Jian Gu^a, Michael Beer^{c,d,e}

^a School of Aerospace Engineering, Xiamen University, Xiamen 361005, R.P. China

^b Faculty of Engineering and Sciences, Universidad Adolfo Ibáñez, Av. Padre Hurtado 750, 2562340 Viña del Mar, Chile

^c Institute for Risk and Reliability, Leibniz Universität Hannover, Callinstr. 34, Hannover, Germany

^d Institute for Risk and Uncertainty, University of Liverpool, Peach Street, L69 7ZF Liverpool, United Kingdom

^e International Joint Research Center for Engineering Reliability and Stochastic Mechanics, Tongji University, Shanghai 200092, China

Abstract

An efficient procedure is proposed to estimate the failure probability function (FPF) with respect to design variables, which correspond to distribution parameters of basic structural random variables. The proposed procedure is based on the concept of an augmented reliability problem, which assumes the design variables as uncertain by assigning a prior distribution, transforming the FPF into an expression that includes the posterior distribution of those design variables. The novel contribution of this work consists of expressing this target posterior distribution as an integral, allowing it to be estimated by means of sampling, and no distribution fitting is needed, leading to an efficient estimation of FPF. The proposed procedure is implemented within three different simulation strategies: Monte Carlo simulation, importance sampling and subset simulation; for each of these cases, expressions for the coefficient of variation of the FPF estimate are derived. Numerical examples illustrate performance of the proposed approaches.

Keywords:

Failure probability function; Bayesian theory; Reliability analysis; Reliability-based optimization

1. Introduction

Reliability and reliability-based design optimization (RBDO) provide useful tools for quantifying uncertainty and performing optimal design under uncertainty, respectively. The application of reliability methods has been widely accepted in structural design, since there are inherent sources of uncertainties affecting the performance of structural systems. RBDO attempts to determine optimal design solutions while explicitly taking into account the effects of uncertainty [1][2]. Note that the failure probability may be highly sensitive to the distribution parameters that characterize basic structural random variables, i.e., mean value or standard deviation. Thus, it is of paramount importance and of great interest to estimate the failure probability as a function of these parameters [3][4]. The latter is particularly true as in several cases, these distribution parameters can be actually interpreted as design variables, as they can represent, for example, the outcome of a fabrication process. Given that the failure probability becomes a function of these distribution parameters / design variables, it is termed within the context of this work as the *Failure Probability Function* (FPF). The FPF can be seen as “reliability sensitivity analysis” that indicates how the failure probability changes with respect to the design variables. Also, the FPF can be used within the context of RBDO, as it allows to decouple the problem into a traditional optimization task without implementing a nested double-loop [5][6].

45 In practice, it is difficult to obtain the FPF with regard to the design parameters, since it usually
46 requires repeated reliability analyses executed at various design parameter values. Even though a
47 variety of methods have been developed to estimate the failure probability of structural systems,
48 performing repeated reliability analyses constitutes still a challenge. In this sense, well established
49 methods for reliability based on approximate analytic representations (e.g., first/second order
50 reliability method - FORM/SORM [7][8]) or simulation methods (such as Monte Carlo simulation
51 [9], importance sampling [10], Subset simulation [11], and Line sampling [12] etc.) still demand
52 computational and numerical efforts which may become remarkable for practical problems,
53 especially when finite element models are involved. As a result, repeated reliability analyses render
54 the direct estimation of FPF computationally intractable.

55 There are many contributions addressing the estimation of the FPF, and a number of methods
56 have been developed, which can be classified into three classes. One class comprises surrogate
57 models. For example, one can build an approximation of the FPF based on design of experiments
58 (DOE). That is, to construct an approximation by selecting some predefined interpolation points in
59 the space of the design parameters. For example, Gasser [13] adopts a pre-defined quadratic
60 function with respect to the design parameters to approximate the logarithm of FPF. Then, a
61 number of reliability analyses are carried out over some interpolation grid points of design
62 parameters, finally to determine the coefficients of the predefined function by a least squares
63 approach. Jensen [14] adopted a linear function to approximate the logarithm of FPF; in this
64 approach, the number of reliability analyses equals that of the design variables. Note that there is
65 a considerable number of surrogate model methods, for example, Kriging method [15][16],
66 Support vector machine [17][18], etc. These methods are widely applied to reliability analysis to
67 approximate the limit state function [19][20], which can be also used to approximate the FPF.
68 However, their practical application may become involved due to the necessity of repeated
69 evaluation of the structural model for training the surrogate. Another variant of surrogate models
70 was proposed by Wei [21][22], that adopted High-dimensional model representation (HDMR) to
71 approximate the FPF within the framework of imprecise stochastic simulation. The second class of
72 approaches for approximating the FPF consists of a post-processing step of a standard reliability
73 analysis. This class of methods focuses on obtaining the FPF with respect to the distribution
74 parameters. For example, Zou [5] expressed the FPF as a linear function of the distribution
75 parameters by applying first-order Taylor series expansion based on the reliability sensitivity
76 information. As the reliability sensitivity is a byproduct of reliability analysis, the FPF can be built
77 by means of a single reliability analysis. Yuan [23] proposed a weighted approach to obtain the FPF.
78 By introducing an instrumental sampling function, the estimate of FPF can be expressed as a
79 function of a set of samples which are generated in a single reliability analysis. Its efficiency
80 depends on the simulation method used, such as, Monte Carlo simulation, importance sampling,
81 Subset simulation. Further, an advanced Line sampling approach is proposed to solve the FPF [24],
82 which is similar with the weighted approach as it only needs one simulation run of line sampling.
83 The third and last class of strategies for estimating the FPF involves the formulation of the reliability
84 problem in an augmented space. Au [25] first consider the design variables as uncertain with an
85 assigned probability distribution. This leads to a reliability problem in an augmented space, which
86 is composed of the basic structural variables and the design parameters. Then, the Bayesian rule is
87 applied to express the FPF as the product of three terms. The key term out of these three is the
88 posterior distribution of the design variables. In this way, the FPF is estimated by performing a
89 single augmented reliability analysis. Ching [26][27] follows the augmented reliability idea and

90 adopted the maximum entropy principle to estimate the posterior distribution of the design
91 variables. Despite all these progresses, there is still a strong need to enhance our ability and
92 efficiency for estimating the FPF for general problems.

93 This contribution proposes an efficient procedure called ‘Augmented space integral’ (ASI) for
94 estimating the structural FPF. In particular, the proposed procedure develops the augmented
95 reliability idea further to handle the FPF with respect to distribution design parameters. The
96 features of the proposed approach are: (1) It is based on the augmented reliability idea [25][26],
97 allowing the FPF to be obtained in a single simulation run and thus, repeated reliability analyses
98 can be avoided; (2) It casts the posterior distribution appearing in the expression of the FPF as an
99 integral, which allows its estimation through simulation by averaging over samples, without need
100 of fitting prescribed probability density functions [25][26]; (3) The work reported here solves the
101 FPF in augmented space, while the weighted approach proposed in [23] is solved in the original
102 random variable space. Thus, the proposed approach can be interpreted as an extended version of
103 the weighted approach.

104 This contribution is organized as follows. In Section 2, the FPF problem and the original
105 augmented reliability method are first briefly given. Then, the mathematical formulation of the
106 proposed procedure is derived, and the implementation with Monte Carlo simulation, importance
107 sampling and Subset simulation are also developed in Section 3. At last, in Section 4, various
108 examples are presented to show the performance of the proposed approach.

110 2. Failure probability function and its estimation in augmented space

111 2.1 Failure probability function definition

112 In this contribution, we focus on the estimation of the FPF with respect to the distribution
113 parameters of basic random variables, such as mean and standard deviation. These distribution
114 parameters could be interpreted as design variables. Note that the failure probability can be highly
115 sensitive to the distribution parameters and thus, it is of great interest to know the relationship of
116 the failure probability with respect to the distribution parameters. This type of problems is
117 encountered, for example, when the mean of the geometrical dimension of a structural member
118 such as thickness, length, height, etc. corresponds to the design variables in reliability-based design
119 optimization.

120 The FPF considered in this contribution is given by

$$P_F(\boldsymbol{\theta}) = \int I_F(\mathbf{x})f(\mathbf{x}|\boldsymbol{\theta})d\mathbf{x} \quad (1)$$

121 where $\mathbf{x} = [x_1, x_2, \dots, x_n]^T$ is the vector of basic random variables of the structure/system;
122 $\boldsymbol{\theta} = [\theta_1, \theta_2, \dots, \theta_{n_\theta}]^T$ is the vector of distribution parameters related with \mathbf{x} ; $f(\mathbf{x}|\boldsymbol{\theta})$ represents
123 the joint conditional Probability Distribution Function (PDF) of \mathbf{x} given $\boldsymbol{\theta}$; $I_F(\mathbf{x})$ is the indicator
124 function, $I_F(\mathbf{x}) = 1$ if $\mathbf{x} \in F$ and $I_F(\mathbf{x}) = 0$, otherwise; $F = \{\mathbf{x}: g(\mathbf{x}) \leq 0\}$ is the failure
125 region and $g(\cdot)$ is the limit state function.

126 Note that there are usually two different types of design variables in structural reliability-
127 based design. One type refers to the variables that affect the limit state function and the other type
128 refers to variables that affect in the distribution parameters of basic random variables [4]. In this
129 contribution, it is found that, when the design variable corresponds to the distribution parameters,
130 the estimator of FPF can be obtained in an efficient way by the proposed procedure. For the sake

131 of simplicity and without loss of generality, it is also assumed that all the basic random variables
 132 are independent with respect to each other.

133 **2.2 Failure probability function transformation in augmented space**

134 The augmented reliability idea provides an efficient means for calculating FPF and was first
 135 proposed by Au [25]. In an augmented space, the design variable θ is no longer a deterministic
 136 quantity but it is modeled as a random variable vector with an instrumental probability distribution
 137 $\varphi(\theta)$. Then, applying the Bayesian theory, the sought failure probability function in Eq. (1) can be
 138 transformed as [25]:

$$P_F(\theta) = \frac{\varphi(\theta|F)P(F)}{\varphi(\theta)} \quad (2)$$

139 where $\varphi(\theta|F)$ is the posterior distribution of θ conditioned on the occurrence of the failure
 140 event; and $P(F)$ is the failure probability of the augmented reliability problem:

$$P(F) = \iint I_F(x)f(x|\theta)\varphi(\theta)dx d\theta \quad (3)$$

141 By virtue of Eq. (2), the FPF is expressed in terms of three components, namely $\varphi(\theta)$, $P(F)$
 142 and $\varphi(\theta|F)$. Among them, $\varphi(\theta)$ can be selected arbitrarily (due to its instrumental nature) and
 143 it is important to note that different distributions for θ do not affect the results of FPF from a
 144 theoretical viewpoint. For example, either Gaussian or Uniform distribution can be employed [26].
 145 However, care should be taken whenever the Gaussian distribution is used, as it may associate
 146 negative values with quantities that are positive due to physical reasons. $P(F)$ can be estimated
 147 by performing reliability analysis in augmented space. The remaining part is to estimate $\varphi(\theta|F)$,
 148 which is the most important and challenging term for the estimation of FPF by means of Eq. (2).
 149 In [25], Au used histograms to represent this term, and latter Ching adopted the maximum entropy
 150 method to approximate the posterior distribution, leading to an estimator for the FPF which is an
 151 explicit expression of θ [26]-[27]. In this contribution, the proposed procedure develops the
 152 augmented reliability method further, such that there is no need to fit a density function to
 153 describe the posterior distribution $\varphi(\theta|F)$.

154 **3. Proposed approach for FPF estimation**

155 As the key for solving the FPF according to Eq. (2) is the assessment of the term $\varphi(\theta|F)$, the
 156 proposed procedure is further developed for handling a particular type of problem where the
 157 design variables are the distribution parameters of basic random variables. It is found that for this
 158 type of problem, the posterior distribution associated with the FPF can be expressed as an integral
 159 which can be estimated by means of samples. Thus, there is no need to fit a probability distribution.
 160 In the following, the proposed procedure, as well as the implementations with three different
 161 simulation approaches are presented.

162 **3.1 Basic formulation of the proposed approach**

163 The proposed procedure attempts to establish a relationship between the posterior
 164 distribution $\varphi(\theta|F)$ and the variable x . If such goal can be fulfilled, then there is no need to fit a
 165 probability distribution in order to estimate $\varphi(\theta|F)$.

166 According to the formula of conditional probability, $\varphi(\theta|F)$ can be developed as:

$$\varphi(\theta|F) = \int \varphi(\theta|x, F)f(x|F)dx = E_{x|F}[\varphi(\theta|x, F)] \quad (4)$$

167 where $E_{x|F}[\cdot]$ means the expectation under $f(x|F)$. Eq. (4) reveals the relationship between the
 168 two posterior distributions, $\varphi(\theta|F)$ and $f(x|F)$. It provides an alternative way to obtain
 169 $\varphi(\theta|F)$, instead of using density fitting methods. According to Eq. (4), if $\varphi(\theta|x, F)$ is obtained
 170 beforehand, then $\varphi(\theta|F)$ can be obtained using simulation, i.e., estimating expectation by the
 171 mean of samples.

172 According to Bayesian theory, $\varphi(\theta|x, F)$ can be simplified to

$$\varphi(\theta|x, F) = \frac{I_F(x)\varphi(\theta|x)}{\int I_F(x)\varphi(\theta|x)d\theta} = I_F(x)\varphi(\theta|x) \quad (5)$$

173 where the term $\varphi(\theta|x)$ can also be rewritten as follows by using Bayesian theory

$$\varphi(\theta|x) = \frac{f(x|\theta)\varphi(\theta)}{f(x)} \quad (6)$$

174 where $f(x)$ is the marginal distribution of x in augmented space (x, θ) which is given by:

$$f(x) = \int f(x, \theta) d\theta = \int f(x|\theta)\varphi(\theta) d\theta \quad (7)$$

175 It has already been stated in [25] that the role of the PDF $\varphi(\theta)$ is not to reflect the uncertainty of
 176 θ . Rather, it is a device to yield information about $P_F(\theta)$ versus θ . The choice of $\varphi(\theta)$ depends
 177 on the region in the design parameter space where $P_F(\theta)$ is to be studied. Without particular
 178 preference for the region to be emphasized, a uniform distribution may be chosen for convenience
 179 [25], i.e., $\theta \sim U[\underline{\theta}, \bar{\theta}]$. In this context, $\varphi(\theta)$ is a constant within $\theta \in [\underline{\theta}, \bar{\theta}]$. Then, the marginal
 180 distribution $f(x)$ can be rewritten as:

$$f(x) = \int_{\underline{\theta}}^{\bar{\theta}} f(x|\theta)\varphi(\theta)d\theta = \varphi(\theta)\Delta(x) \quad (8)$$

181 where $\Delta(x) = \int_{\underline{\theta}}^{\bar{\theta}} f(x|\theta)d\theta$ is an integral over the design region. Further details on the
 182 calculation of $\Delta(x)$ are presented in Appendix A.

183 Substitution of Eq. (8) into (6) allows determining the sought the posterior distribution
 184 $\varphi(\theta|x)$, which is equal to:

$$\varphi(\theta|x) = \frac{f(x|\theta)\varphi(\theta)}{f(x)} = \frac{f(x|\theta)}{\Delta(x)} \quad (9)$$

185 Replacing Eqs. (5) and (9) into Eq. (4) leads to:

$$\varphi(\theta|F) = \int I_F(x) \frac{f(x|\theta)}{\Delta(x)} f(x|F) dx = E_{x|F} \left[\frac{f(x|\theta)}{\Delta(x)} \right] \quad (10)$$

186 And $f(x|F)$ is the PDF of x conditional on F , which is given by:

$$f(x|F) = \frac{I_F(x)f(x)}{\int I_F(x)f(x) dx} = \frac{I_F(x)f(x)}{\int I_F(x) \int f(x, \theta) d\theta dx} = \frac{I_F(x)f(x)}{P(F)} \quad (11)$$

187 Substitution of Eq. (11) into Eq. (10) allows rewriting $\varphi(\theta|F)$ as:

$$\varphi(\theta|F) = \frac{1}{P(F)} \int \frac{I_F(x)f(x|\theta)}{\Delta(x)} f(x) dx \quad (12)$$

188 Finally, substitution of Eq. (12) into Eq. (2) leads to the final expression for the FPF, which
 189 can be expressed as:

$$P_F(\theta) = \frac{1}{\varphi(\theta)} \int \frac{I_F(x)f(x|\theta)}{\Delta(x)} f(x) dx = \frac{1}{\varphi(\theta)} E_x \left[\frac{I_F(x)f(x|\theta)}{\Delta(x)} \right] \quad (13)$$

190 where $E_x[\cdot]$ represents expectation under the marginal distribution $f(x)$.

191

192 3.2 Proposed procedure based on Monte Carlo simulation

193 After a general formula for the FPF has been obtained above, it can be implemented by means
 194 of a simulation-based method. The most direct approach is using Monte Carlo simulation. In the
 195 following, the proposed procedure based on Monte Carlo simulation is presented, which is
 196 denoted as 'ASI-MCS' for compactness.

197 Note that contrary to traditional reliability analysis, the augmented reliability problem must
 198 be solved in the augmented space $(\mathbf{x}, \boldsymbol{\theta})$. According to Eq. (13), if $P_F(\boldsymbol{\theta})$ is solved by using
 199 Monte Carlo Simulation, the key is to generate samples from \mathbf{x} which follow the marginal
 200 distribution of $f(\mathbf{x})$. However, in a general case, one may not sample directly from $f(\mathbf{x})$, as it may
 201 not correspond to a known probability distribution. However, the following workaround can be
 202 implemented. First, generate samples $\{\boldsymbol{\theta}^{(j)}, j = 1, \dots, N\}$ that follow $\varphi(\boldsymbol{\theta})$. Then, for each of
 203 these samples, generate samples $\{\mathbf{x}^{(j)}, j = 1, \dots, N\}$, each of them distributed according to
 204 $f(\mathbf{x}|\boldsymbol{\theta}^{(j)})$. Thus, the set of samples $\{(\mathbf{x}^{(j)}, \boldsymbol{\theta}^{(j)}), j = 1, \dots, N\}$ follows $f(\mathbf{x}, \boldsymbol{\theta})$. Ignoring the
 205 samples associated with $\boldsymbol{\theta}$, then $\{\mathbf{x}^{(j)}, j = 1, \dots, N\}$ are distributed as $f(\mathbf{x})$.

206 According to Eq. (10), the estimator for the posterior distribution is given by:

$$\hat{\varphi}(\boldsymbol{\theta}|F) = \frac{1}{N_F} \sum_{j=1}^{N_F} \frac{f(\mathbf{x}^{(j)}|\boldsymbol{\theta})}{\Delta(\mathbf{x}^{(j)})} \quad (14)$$

207 This implies that, instead of using distribution fitting approach to estimate $\varphi(\boldsymbol{\theta}|F)$ (as
 208 performed in [26]), the proposed approach can estimate directly the $\varphi(\boldsymbol{\theta}|F)$ by means of
 209 sampling.

210 According to Eq. (13), the FPF $P_F(\boldsymbol{\theta})$ is estimated as:

$$\hat{P}_F(\boldsymbol{\theta}) = \frac{1}{\varphi(\boldsymbol{\theta})} \frac{1}{N} \sum_{j=1}^N \frac{I_F(\mathbf{x}^{(j)})f(\mathbf{x}^{(j)}|\boldsymbol{\theta})}{\Delta(\mathbf{x}^{(j)})} \quad (15)$$

211 It is obvious that the estimator $\hat{P}_F(\boldsymbol{\theta})$ is unbiased, and its variance can be readily obtained
 212 as:

$$Var[\hat{P}_F(\boldsymbol{\theta})] \approx \frac{1}{N-1} \left\{ \frac{1}{N} \sum_{j=1}^N \left\{ \frac{I_F(\mathbf{x}^{(j)})f(\mathbf{x}^{(j)}|\boldsymbol{\theta})}{\varphi(\boldsymbol{\theta})[\Delta(\mathbf{x}^{(j)})]} \right\}^2 - \hat{P}_F^2(\boldsymbol{\theta}) \right\} \quad (16)$$

213 And the Coefficient of variation (C.o.v.) of $\hat{P}_F(\boldsymbol{\theta})$ is given by:

$$Cov[\hat{P}_F(\boldsymbol{\theta})] = \frac{\sqrt{Var[\hat{P}_F(\boldsymbol{\theta})]}}{E[\hat{P}_F(\boldsymbol{\theta})]} \approx \frac{\sqrt{Var[\hat{P}_F(\boldsymbol{\theta})]}}{\hat{P}_F(\boldsymbol{\theta})} \quad (17)$$

214

215 3.3 Proposed procedure based on importance sampling

216 The proposed procedure can be also implemented with importance sampling, which is
 217 denoted as 'ASI-IS'. Introducing an appropriate importance sampling function $H(\mathbf{x})$ in augmented
 218 space, the FPF in Eq. (13) can be rewritten as:

$$P_F(\boldsymbol{\theta}) = \frac{1}{\varphi(\boldsymbol{\theta})} \int \frac{I_F(\mathbf{x})f(\mathbf{x}|\boldsymbol{\theta})}{\Delta(\mathbf{x})} \frac{f(\mathbf{x})}{H(\mathbf{x})} H(\mathbf{x}) d\mathbf{x} \quad (18)$$

219 Substitution of Eq. (8) into (18) allows rewriting $P_F(\boldsymbol{\theta})$ as:

$$P_F(\boldsymbol{\theta}) = \int \frac{I_F(\mathbf{x})f(\mathbf{x}|\boldsymbol{\theta})}{H(\mathbf{x})}H(\mathbf{x})d\mathbf{x} = E_H \left[\frac{I_F(\mathbf{x})f(\mathbf{x}|\boldsymbol{\theta})}{H(\mathbf{x})} \right] \quad (19)$$

220 where $E_H[\cdot]$ denotes the expectation under $H(\mathbf{x})$.

221 It should be noted that the final expression in Eq. (19) is the same as the one associated with
 222 weighted importance sampling introduced in a previous work [23], but its meaning is quite
 223 different. In the previous work, everything is formulated in the space associated with \mathbf{x} , but in the
 224 present contribution, it is solved in the augmented space $(\mathbf{x}, \boldsymbol{\theta})$. Thus, in this sense, it can be seen
 225 as an extended version of the previous work.

226 The importance sampling density $H(\mathbf{x})$ should be selected properly. There are plenty of
 227 contributions addressing the way of determining importance sampling density. However, few of
 228 them address how to determine such density in an augmented space. Here, we present some
 229 suggestions. There are two ways for determining $H(\mathbf{x})$ in augmented space. One is based on a
 230 design point \mathbf{x}^* . The design point can be solved according to a nominal value of design parameter,
 231 say, $\boldsymbol{\theta}_0$, which can be simply set as the center of the domain associated with $\boldsymbol{\theta}$, i.e., $\boldsymbol{\theta}_0 = (\underline{\boldsymbol{\theta}} +$
 232 $\bar{\boldsymbol{\theta}})/2$. Alternatively, the design point can be obtained by searching the point \mathbf{x}^* in the augmented
 233 space which has the largest joint PDF value $f(\mathbf{x}, \boldsymbol{\theta})$ and that belongs to the failure domain F . For
 234 this purpose, the random variables can be classified into two types, that is, $\mathbf{x} = [\mathbf{x}_\theta, \mathbf{x}_r]$, where
 235 \mathbf{x}_θ is the variable vector related with design parameters $\boldsymbol{\theta}$ and \mathbf{x}_r is the vector of the rest of
 236 random variables (whose distribution is not affected by $\boldsymbol{\theta}$). Then, based on the design point $\mathbf{x}^* =$
 237 $[\mathbf{x}_\theta^*, \mathbf{x}_r^*]$, $H(\mathbf{x})$ can be chosen as

$$H(\mathbf{x}) = f(\mathbf{x}_\theta)H(\mathbf{x}_r|\mathbf{x}_\theta^*) \quad (20)$$

238 where $f(\mathbf{x}_\theta)$ is the marginal distribution for \mathbf{x}_θ given in Eq. (8).

239 The other way to choose $H(\mathbf{x})$ is based on adaptive importance sampling density [29]. That
 240 is, to establish an approximate optimal density. For example, we can pre-sample in the failure
 241 region (in augmented space), and then, based on these samples, obtain an approximated sampling
 242 density.

243 Suppose $H(\mathbf{x})$ has been chosen, then samples can be generated according to $H(\mathbf{x})$.
 244 Suppose a total of N samples are generated, $\{\mathbf{x}^{(j)}, j = 1, \dots, N\}$. Then according to Eq. (19),
 245 $P_F(\boldsymbol{\theta})$ is estimated as:

$$\hat{P}_F(\boldsymbol{\theta}) = \frac{1}{N} \sum_{j=1}^N \frac{I_F(\mathbf{x}^{(j)})f(\mathbf{x}^{(j)}|\boldsymbol{\theta})}{H(\mathbf{x}^{(j)})} \quad (21)$$

246 It is obvious that the estimator $\hat{P}_F(\boldsymbol{\theta})$ is unbiased, and its variance is obtained as

$$Var[\hat{P}_F(\boldsymbol{\theta})] \approx \frac{1}{N-1} \left\{ \frac{1}{N} \sum_{j=1}^N \left\{ \frac{I_F(\mathbf{x}^{(j)})f(\mathbf{x}^{(j)}|\boldsymbol{\theta})}{H(\mathbf{x}^{(j)})} \right\}^2 - \hat{P}_F^2(\boldsymbol{\theta}) \right\} \quad (22)$$

247 And the C.o.v. of $\hat{P}_F(\boldsymbol{\theta})$ is given by:

$$Cov[\hat{P}_F(\boldsymbol{\theta})] = \frac{\sqrt{Var[\hat{P}_F(\boldsymbol{\theta})]}}{E[\hat{P}_F(\boldsymbol{\theta})]} \approx \frac{\sqrt{Var[\hat{P}_F(\boldsymbol{\theta})]}}{\hat{P}_F(\boldsymbol{\theta})} \quad (23)$$

248

249 3.4 Proposed procedure based on Subset simulation

250 In this section, Subset simulation is adopted and integrated within the proposed procedure,

251 which is denoted as ‘ASI-SS’. Subset simulation is an efficient approach for evaluating the failure
 252 probability of general reliability problems, and is especially suitable for high dimensional, low
 253 failure probability reliability problems [11]. The basic idea of Subset simulation is that a low failure
 254 probability event is expressed as the product of a series of conditional, larger probabilities, whose
 255 estimation is straightforward. The proposed ASI procedure can be implemented by using Subset
 256 Simulation, as described in the following.

257 Let $F_1 \supset F_2 \supset \dots \supset F_m = F$ be a nested sequence of failure events in subset simulation in
 258 augmented space $(\mathbf{x}, \boldsymbol{\theta})$ where $F_i = \{g(\mathbf{x}) \leq b_i\} (i = 1, 2, \dots, m)$; then the failure probability
 259 can be expressed by

$$P(F) = P(F_1) \prod_{i=2}^m P(F_i|F_{i-1}) \quad (24)$$

260 Note that b_1, b_2, \dots, b_{m-1} are the intermediate threshold values which are adaptively determined,
 261 so that the corresponding probabilities $P(F_1), P(F_2|F_1), \dots, P(F_{m-1}|F_{m-2})$ can be all set to be
 262 p_0 , e.g., $p_0 = 0.1$ for convenience. The final threshold $b_m = 0$ is not chosen adaptively.

263 Suppose there are N_s samples generated at (m-1)th level. Moreover, it is considered that
 264 there are a number of N_F failure samples located in the final level (target failure region F),
 265 $\{(\mathbf{x}^{(j)}, \boldsymbol{\theta}^{(j)}), j = 1, \dots, N_F\}$, which are distributed as $f(\mathbf{x}, \boldsymbol{\theta}|F)$. Ignoring the $\boldsymbol{\theta}$ part, the samples
 266 $\{\mathbf{x}^{(j)}, j = 1, \dots, N_F\}$ are distributed as $f(\mathbf{x}|F)$. Then according to Eq. (10), $\varphi(\boldsymbol{\theta}|F)$ can be
 267 estimated by

$$\hat{\varphi}(\boldsymbol{\theta}|F) = \frac{1}{N_F} \sum_{j=1}^{N_F} \frac{f(\mathbf{x}^{(j)}|\boldsymbol{\theta})}{\Delta(\mathbf{x}^{(j)})} \quad (25)$$

268 This means that the distribution $\varphi(\boldsymbol{\theta}|F)$ can be estimated using simulation, and no distribution
 269 fitting is required. The failure probability in Eq. (24) can be estimated by

$$\hat{P}(F) = p_0^{m-1} \frac{N_F}{N_s} \quad (26)$$

270 Finally, substitution of Eqs. (25) and (26) into (2) leads to the following expression for FPF
 271 $P_F(\boldsymbol{\theta})$:

$$\hat{P}_F(\boldsymbol{\theta}) = \frac{p_0^{m-1}}{\varphi(\boldsymbol{\theta})} \frac{1}{N_s} \sum_{j=1}^{N_s} \frac{I_F(\mathbf{x}^{(j)}) f(\mathbf{x}^{(j)}|\boldsymbol{\theta})}{\Delta(\mathbf{x}^{(j)})} = \frac{p_0^{m-1} \hat{P}_m(\boldsymbol{\theta})}{\varphi(\boldsymbol{\theta})} \quad (27)$$

272 where

$$\hat{P}_m(\boldsymbol{\theta}) = \frac{1}{N_s} \sum_{j=1}^{N_s} \frac{I_F(\mathbf{x}^{(j)}) f(\mathbf{x}^{(j)}|\boldsymbol{\theta})}{\Delta(\mathbf{x}^{(j)})} \quad (28)$$

273 And the C.o.v. of $\hat{P}_F(\boldsymbol{\theta})$ can be approximated by:

$$Cov[\hat{P}_F(\boldsymbol{\theta})] = \sqrt{\sum_{i=1}^m \frac{Var(\hat{P}_i)}{P_i^2}} \approx \sqrt{\sum_{i=1}^m \frac{Var(\hat{P}_i)}{\hat{P}_i^2}} \quad (29)$$

274 A detailed derivation of Eq. (29) is given in Appendix B.

275

276 **3.5 Comparison of different approaches**

277 Table 1 presents the comparison of different approaches that can produce an estimate of the
 278 FPF by means of a single reliability analysis.

279 In Table 1, ‘ASI’ refers to the proposed procedure herein; ‘WA’ refers to the Weighted
 280 Approaches previously proposed by the author, which includes Weighted Monte Carlo Simulation
 281 (WMCS), Weighted importance sampling (WIS) and Weighted Subset simulation (WSS); ‘ALS’ refers
 282 to Advanced Line Sampling method. ‘Au’ refers to the augmented reliability idea proposed by Au;
 283 ‘Ching’ refers to the advanced augmented reliability idea with maximum entropy; ‘Wei’ refers to
 284 non-intrusive imprecise stochastic simulation for uncertainty propagation.

285 Table 1. Comparison of different approaches

Methods	Space	Expression	Simulation	Design variable
ASI	Augmented space	Integral	MCS, IS, SS	Distribution parameter
WA[23]	Original space	Integral	MCS, IS, SS	Distribution parameter
ALS[24]	Original space	Integral	Line sampling	Distribution parameter
Au[25]	Augmented space	Histogram	SS	Distribution parameter or deterministic parameter
Ching[26]	Augmented space	Maximum entropy	SS	Distribution parameter or deterministic parameter
Wei[21]	Augmented space	Integral	MCS, SS	Distribution parameter

286
 287 Among these methods, WA and ALS are carried out in original space of basic random variables,
 288 while the other methods are all formulated in augmented space. In Au and Ching, the estimator of
 289 FPF is finally expressed by using histogram or by using maximum entropy estimation. However,
 290 they can handle both the distribution parameters and design variables affecting the limit state
 291 function, whereas other approaches only handle the former one. The proposed approach
 292 preserves the advantage of using only a single reliability simulation in augmented space.
 293 Furthermore, it does not need to estimate the conditional distribution $\varphi(\theta|F)$ by using density
 294 approximation (considering, e.g. maximum entropy principle) and in addition, there is no need to
 295 select the shape of the probability density function.

296 Thus, in summary, the proposed procedure can be seen as a particular version of the
 297 augmented reliability idea (Au and Ching), which improves the efficiency when handling the FPF
 298 with respect to distribution parameters, resulting in better performance. Also, the proposed
 299 procedure can be seen as a further advanced version of the weighted approach (Yuan), which
 300 extends the original space to the augmented space, resulting in a better improvement on accuracy.
 301 These characteristics will be shown in the examples given in Section 4.

302

303 **3.6 Procedure of the proposed approach**

304 The procedure of the proposed approach is summarized as follows.

305 1) Choose a distribution $\varphi(\theta)$.

306 For general cases, uniform distribution may be chosen.

307 2) Carry out the simulation in augmented space.

308 ASI-MCS, ASI-IS or ASI-SS can be selected to carry out reliability analysis in the augmented

309 space $(\mathbf{x}, \boldsymbol{\theta})$, producing failure samples $\{(\mathbf{x}^{(j)}, \boldsymbol{\theta}^{(j)}): j = 1, \dots, N_F\}$.

310 3) Obtain the FPF estimator

311 The FPF can be obtained according to Eq. (15) for ASI-MCS, Eq. (21) for ASI-IS or (27) for
312 ASI-SS; their respective C.o.v.'s can be calculated as well according to Eq. (17) for ASI-MCS, Eq.
313 (23) for ASI-IS or (29) for ASI-SS.

314

315 4. Examples

316 In order to verify the feasibility and accuracy of the proposed approaches (ASI-MCS, ASI-IS and
317 ASI-SS), numerical and practical engineering examples are presented in this section. Meanwhile,
318 different methods are also used for comparison purposes. 'Direct MCS' refers to the results
319 obtained by Direct MCS, which can be seen as the reference results. 'WMCS' refers to
320 the 'Weighted Monte Carlo simulation' method [23]; 'WIS' refers to the 'Weighted Importance
321 sampling' method [23]. Note that in the proposed procedure, the prior distribution is selected as
322 a uniform distribution for all the examples.

323 4.1 Example 1: A test example

324 The first example considers a simple limit state function, which is given by:

$$g(\mathbf{x}) = e^{0.04x_1+7} - e^{0.3x_1^2+5} * x_2 \quad (30)$$

325 where $\mathbf{x} = [x_1, x_2]$, x_1 and x_2 are independent, Gaussian distributed random variables, such
326 that $x_1 \sim N(\theta, 0.5)$, $x_2 \sim N(0, 0.5)$; the mean of x_1 is taken as the design parameter, and the
327 design domain is $\theta \in [-2, 2]$.

328 The proposed ASI approaches (ASI-MCS, ASI-IS and ASI-SS) are applied to this toy problem.
329 For comparison, the weighted approaches (WMCS, WIS and WSS) [23] and GEMCS in [21] are also
330 applied. The computational cost for these approaches is listed in Table 2. Note that for the
331 application of all of these methods, a single reliability analysis is required to obtain the FPF and its
332 corresponding C.o.v. In addition, the direct MCS is carried out in ten independent simulation runs
333 to generate point wise failure probability estimates, which are regarded as the exact reference
334 results. The obtained FPF results (according to Eq. (15) for ASI-MCS, Eq. (21) for ASI-IS or (27)
335 for ASI-SS) and C.o.v. of the estimate (according to Eq. (17) for ASI-MCS, Eq. (23) for ASI-IS or (29)
336 for ASI-SS.) are given in Fig. 1 and Fig. 2, respectively.

337 Note that for the implementation of ASI-MCS, a total of 10^5 samples are generated, and 143
338 failure samples fall within the failure domain; whereas WMCS was implemented considering 10^9
339 samples, with a nominal setting $\theta_0 = 0$, and only 50 failure samples are obtained. This is due to
340 the fact that the proposed ASI approaches are implemented in augmented space where it is
341 assumed $\theta \sim U[-2, 2]$, and the corresponding augmented failure probability is larger than the one
342 where it is assumed that $\theta_0 = 0$. It can be seen from Fig. 1 that both ASI-MCS and WMCS obtained
343 quite accurate FPF results (consistent with the reference results provided by Direct MCS). However,
344 the samples used for WMCS are $1000 (=10^9/10^5)$ times larger than that of ASI-MCS. In this sense,
345 the proposed ASI-MCS overperforms the WMCS in terms of efficiency. Compared with GEMCS, the
346 proposed approach is more accurate (see Fig. 1) and more robust, as the C.o.v. of estimate by
347 GEMCS vary drastically (see Fig. 2).

Table 2. Comparisons of different methods for Example 1

Methods	No. of samples	No. of failure samples
ASI-MCS	10^5	163
ASI-IS	2000	61
ASI-SS	200×4*	185
WMCS	10^9	50
WIS	2000	962
WSS	500×9	258
GEMCS	10^5	135
Direct MCS	$10^8 \times 10$	

349 *: "200×4" means 200 samples are used for each level and a total of 4 levels are used.

350

351

352

353

354

355

356

357

358

359

360

361

362

363

364

365

366

367

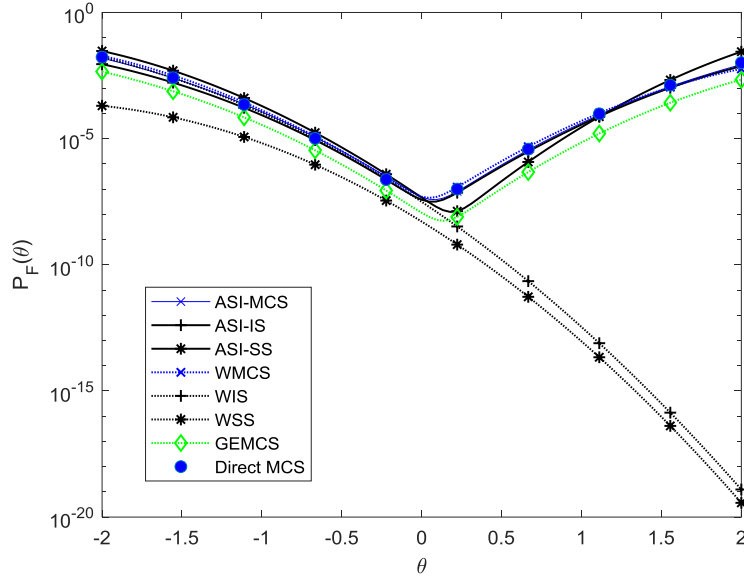
368

369

370

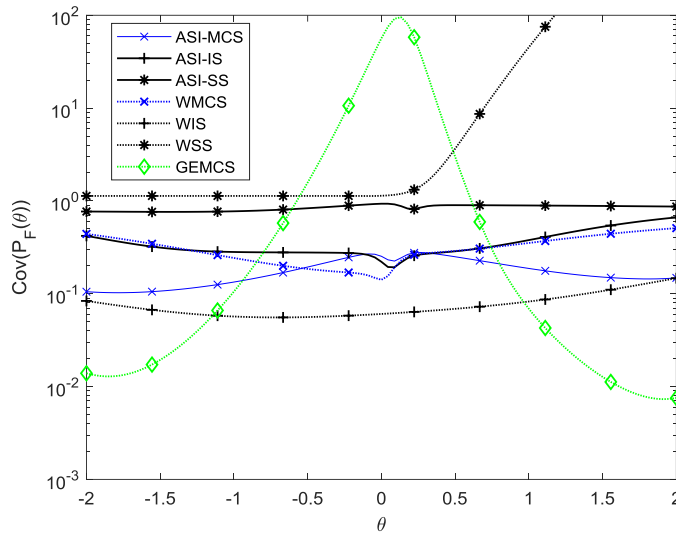
371

ASI-IS is applied such that the sampling function is constructed based on the design point. The design point $\mathbf{x}^* = [-2.35, 1.26]$ is found when assuming $\theta_0 = 0$. Then, the sampling function setting for ASI-IS is $H(\mathbf{x}) = f(x_1)H(x_2|\mathbf{x}_1^*)$. A number of $N=2000$ samples are generated to estimate the FPF. Meanwhile, WIS is also applied. The instrumental sampling function for WIS is Gaussian distributed and centered on design point \mathbf{x}^* [23]. Note that, the difference between ASI-IS and WIS is that they are carried out in different spaces, i.e., augmented space and original space, respectively, so they obtain different numbers of failure samples. From Fig. 1, it can be seen that the FPF obtained by ASI-IS matches quite well the reference values. However, the result by WIS possesses considerable error when $\theta \in [0.5, 2]$. The reason is illustrated in Fig. 3 which shows the failure samples generated by the different approaches. It is clearly seen that the failure samples generated by WIS are located in one important region, while the region corresponding to $x_1 \in [2, 3]$ contains no samples. Note that this region will be the importance failure region when $\theta \in [0.5, 2]$. Failure in exploring this region leads to underestimate the FPF over $\theta \in [0.5, 2]$. The proposed ASI-IS can overcome this disadvantage, as it can generate failure samples in both important regions (see Fig. 3). A similar phenomenon can be seen in the figures related with ASI-SS and WSS. The reason behind this is that, the proposed approach can explore all the important failure regions (corresponding to different values of $\theta \in [\theta, \bar{\theta}]$) by sampling in the augmented space, while the weighted approach may just concentrate in an important failure region corresponding to $\theta = \theta_0$. Thus, the superiority of accuracy and robustness of the proposed approach over the weighted approach are well demonstrated through this example.



372
373

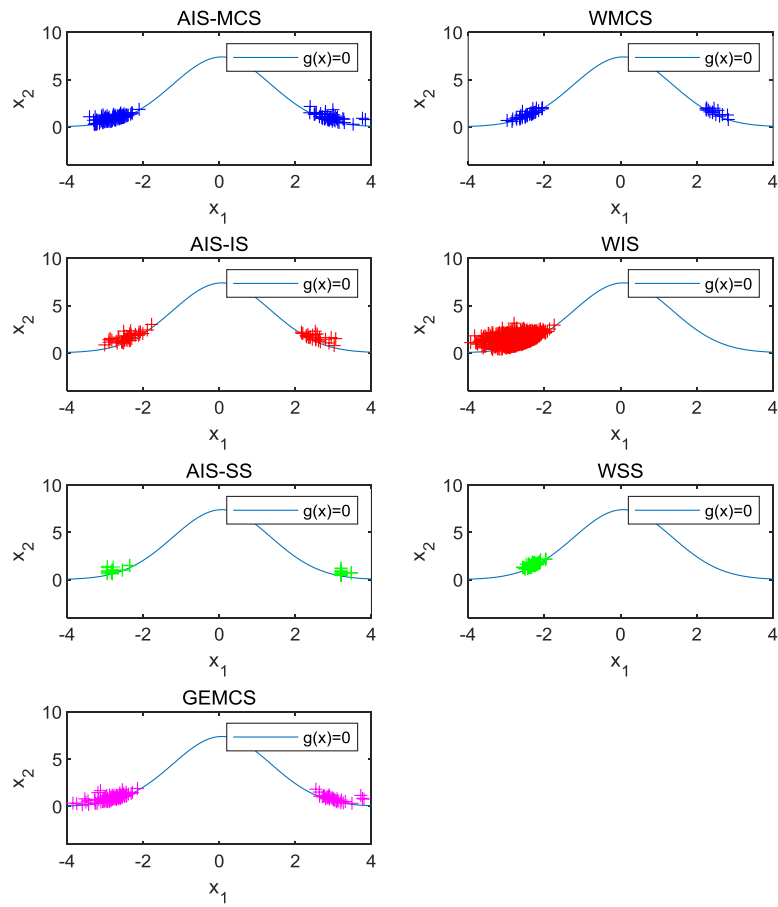
Fig. 1. FPF results obtained by different approaches for Example 1



374
375
376

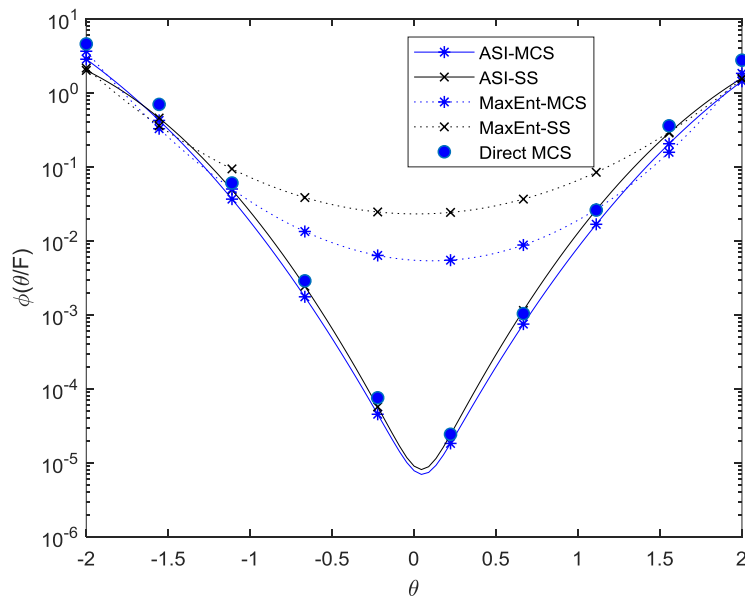
Fig. 2. The C.o.v.'s of FPF results obtained by different approaches for Example 1

377 Also, the proposed ASI procedure is compared with the maximum entropy estimation which
378 is used in [26]. Fig. 4 shows the posterior distribution $\varphi(\theta|F)$ obtained by these methods.
379 'MaxEnt-MCS' and 'MaxEnt-SS' refer to the approaches that use Maximum Entropy estimate to fit
380 the target distribution based the failure samples generated from MCS and SS, respectively. Note
381 that the same set of samples are used for different approaches, i.e., both ASI-MCS and MaxEnt-
382 MCS use the same set of 163 failure samples, while both ASI-SS and MaxEnt-SS use the same set
383 of 183 failure samples. It can be seen that the results by the proposed ASI-MCS and ASI-SS are
384 consistent with the reference result. However, the results by the maximum entropy estimation
385 have remarkable errors in this example. Note that as there are less than 200 failure samples,
386 methods based on distribution fitting may lead to considerable errors. On the contrary, the
387 proposed procedure actually calculates an integral by means of sampling and accurate estimates
388 can be obtained. Therefore, the advantages on accuracy and efficiency of the proposed procedure
389 have been clearly shown.



390
391

Fig. 3. The failure samples generated by different approaches for Example 1



392
393
394

Fig. 4. The distribution $\varphi(\theta|F)$ obtained by different approaches for Example 1

395 **4.2 Example 2: Automobile front axle**

396 Front axle is an important component of automobile that bears heavy loads [31] (Fig. 5). An I-
 397 beam is often used in the design of front axle due to its high bend strength and light weight. As
 398 shown in Fig. 5, a critical component of the axle is located in the I-beam part. To test the static
 399 strength of the front axle, the limit-state function can be expressed as

400
$$g(\mathbf{x}) = \sigma_s - \sqrt{\sigma^2 + 3\tau^2} \quad (31)$$

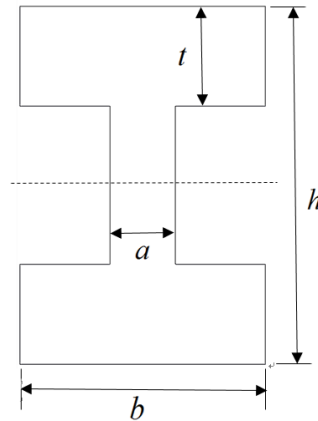
401 where σ_s is the limit-state stress associated with yielding. According to the material property of
 402 the front axle, the limit stress of yielding σ_s is 680 MPa. The maximum normal stress and shear
 403 stress are $\sigma = M/W_x$ and $\tau = T/W_p$, where M and T are bending moment and torque,
 404 respectively, W_x and W_p are section factor and polar section factor, respectively, which are given
 405 as [32]

406
$$W_x = \frac{a(h-2t)^3}{6h} + \frac{b}{6h}[h^3 - (h-2t)^3] \quad (32)$$

407
$$W_p = 0.8bt^2 + 0.4[a^3(h-2t)/t] \quad (33)$$

408 The geometry variables of I-beam a , b , t , h and the load M and T are independent variables
 409 with distribution parameters listed in Table 3. Note that all the variables are restricted to positive
 410 value due to physical reason, actually they are all truncated variables.

411



412

413

414

415

Fig. 5. Diagram of automobile front axle

Table 3. The distribution information of the random variables in Example 2

Random variable	a (mm)	t (mm)	b (mm)	h (mm)	M (KN·m)	T (KN·m)
Location parameter	$\theta_1 = \mu_a$	$\theta_3 = \mu_t$	65	85	3.65	$\theta_4 = \mu_T$
Scale parameter	$\theta_2 = \sigma_a$	1.5	6.5	8.5	0.27	0.24
Distribution	Normal	Normal	Normal	Normal	Gumbel	Gumbel

416

417 The design parameters given in Table 3 include the mean value and standard deviation of the
 418 normal variable, and also the location parameter of the non-normal distributed variable. The
 419 design domains are $\theta_1 = \mu_a \in [11, 15]$ mm, $\theta_2 = \mu_t \in [0.8, 1.6]$ mm, $\theta_3 = \mu_t \in [12, 18]$ mm
 420 and $\theta_4 = \mu_T \in [2.8, 3.8]$ KN·m, respectively.

421

422

Table 4. Comparisons of different methods for Example 2

Methods	No. of samples	No. of failure samples
ASI-MCS	10^5	825
ASI-IS	3000	107
ASI-SS	1000×3	790
WMCS	10^5	38
WIS	3000	1371
WSS	1000×4	310
Direct MCS	$10^6 \times 10$	-

423

424

The FPF is estimated by means of the proposed approaches, ASI-MCS, AIS-IS and AIS-SS. For comparison, the weighted approaches, WMCS, WIS and WSS are also applied. In addition, direct MCS is carried out considering ten independent simulation runs to generate point wise failure probability estimates which are regarded as the reference results.

426

427

428

Fig. 6 shows the FPF results obtained by different approaches. Note that the FPF is a four-dimensional function, and in the figure, the FPF with respect to each dimension is shown (while others are fixed at the center values of the design intervals). Information on the implementation details for each approach is listed in Table 4. It is seen from the figure that the results by the proposed approaches are in good agreement with the reference results (denoted by dots).

429

430

431

432

433

434

435

436

437

438

439

440

441

442

443

444

445

446

447

AIS-MCS is implemented considering a total of $N = 10^5$ samples, and $N_F = 825$ failure samples are obtained. Whereas WMCS also involves 10^5 samples and only $N_F = 38$ failure samples are obtained. The reason is that AIS-MCS is carried out in the augmented space which owns a bigger failure probability than that of WMCS. A similar situation happens when comparing AIS-SS and WSS. WSS is applied with $N = 1000 \times 4$ samples (1000 for each of the 4 levels considered). While the proposed ASI-SS uses only $N = 1000 \times 3$ samples to obtain a satisfactory estimate of FPF. Computation can be saved when considering the formulation in the augmented space by AIS-MCS and AIS-SS. The results by the weighted approaches possess remarkable errors in this example. For instance, a large error exists when $\theta_2 \in [1, 1.6]$ and also $\theta_4 \in [3.6, 3.8]$. The reason behind such error is that, since the sampling function of the weighted approach is centered in the midpoint of the design region, it cannot cover the important failure region in the original space sufficiently well as the proposed ASI approaches do. In conclusion, from the figure and table, the results obtained shows that the proposed approaches are applicable for multiply-dimension design parameters and for both the normal and non-normal variables, also showing more accuracy than other approaches.

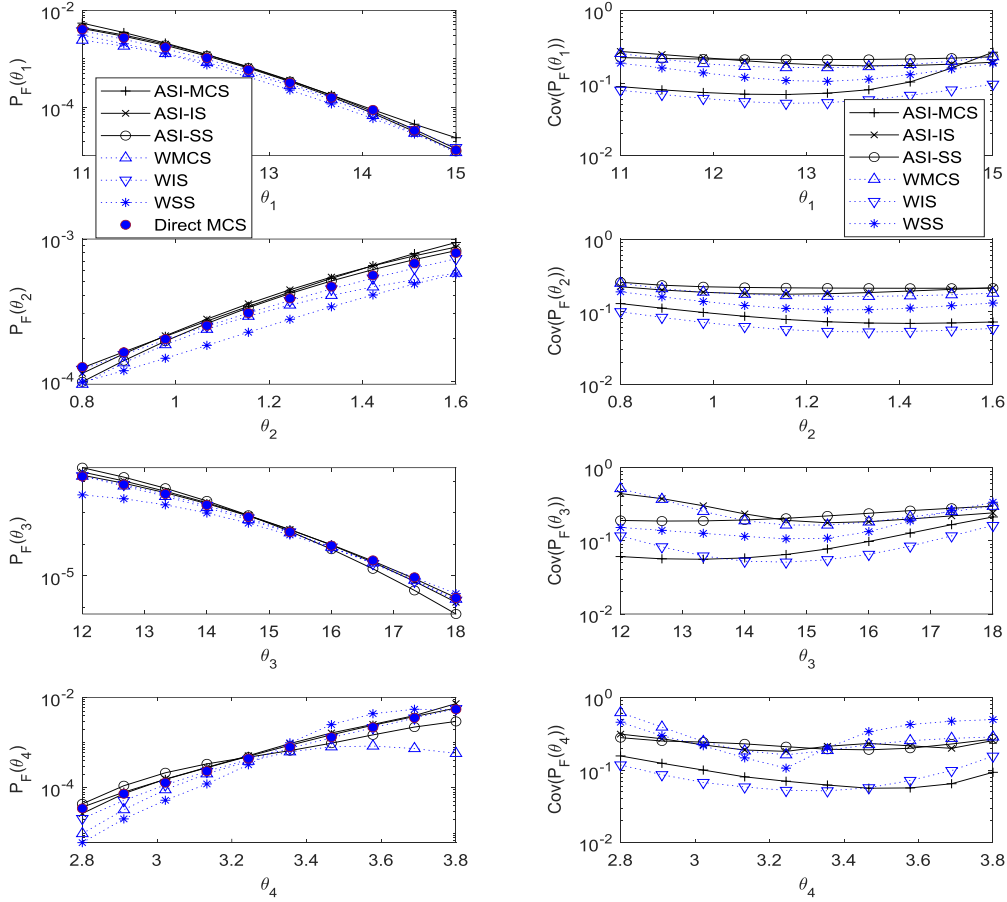


Fig. 6. The FPF estimates obtained by the different methods for Example 2

448

449

450

451

4.3 Example 3: Steel frame subject to stochastic acceleration

452

4.3.1 General model introduction

453

Consider a six-story steel frame as shown in Fig. 7, which has been previously investigated in [23]. This structure is assumed to have rigid floors and behave within the linear-elastic range, with classical damping. The damping ratio of the i -th mode is denoted as $\zeta_i (i = 1, \dots, 6)$. Linear viscous damping elements, called passive dampers, are installed as diagonal bracings. The damping coefficient of the damper in the i -th ($i = 1, \dots, 6$) story is denoted as C_{di} and their values can be adjusted. In this example, the damping coefficient of each damper $C_{di} (i = 1, \dots, 6)$, the original modal damping ratios of the building, $\zeta_i (i = 1, \dots, 6)$, the stiffness of each story, $k_i (i = 1, \dots, 6)$, and the mass of each story, $m_i (i = 1, \dots, 6)$, are considered as (truncated) Gaussian variables. The corresponding distribution information of these 24 structural random variables is given in Table 5.

462

Stochastic ground acceleration $\ddot{a}_g(t)$ which is modeled as Gaussian white noise $W(t)$ is applied to this the structure. When the peak interstory drift ratio over any of the stories of the structure exceeds a threshold level b , structural failure occurs. The damage level $b=1.5\%$ (Life-Safety) is considered herein. A duration of $T = 10s$ and time interval of $\Delta t = 0.05s$ are assumed. The discrete approximation for $W(t)$ is applied at time instants $t_k = k\Delta t (k = 1, 2, \dots, n_t)$, i.e., $W(t_k) = Z(t_k)\sqrt{2\pi S/\Delta t}$ where $S = 0.05m^2/s^3$ is the spectral intensity and $Z_k = Z(t_k)$ are independent identical distributed Gaussian random variables, thus there are $n_k = k/\Delta t = 200$ input random variables.

469

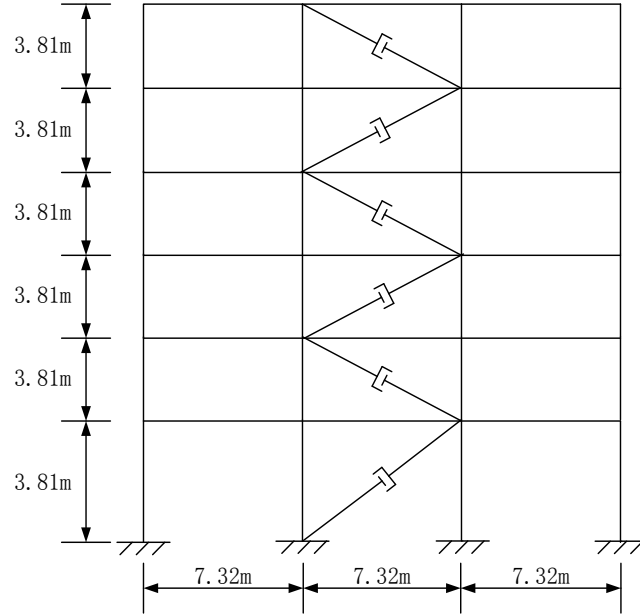


Fig. 7. Six-story steel frame structure with passive dampers

Here, the mean values of the first story stiffness is taken as the design parameter, i.e., $\theta = \mu_{k_1}$, and the design interval for θ is [100, 200] (kN/mm). The reason for considering the mean value of the first story is that in practical situations, it dominates the calculation of the failure probability (see, e.g. [34]).

Table 5. Distribution information of structural random variables

Variable	Mean	C.o.v.
k_1 (kN/mm)	$\theta = \mu_{k_1} \in [100, 200]$	0.1
k_2 (kN/mm)	367	0.1
k_3 (kN/mm)	246	0.1
k_4 (kN/mm)	246	0.1
k_5 (kN/mm)	175	0.1
k_6 (kN/mm)	175	0.1
m_1 (ton)	283	0.1
m_2 (ton)	263	0.1
m_3 (ton)	256	0.1
m_4 (ton)	255	0.1
m_5 (ton)	247	0.1
m_6 (ton)	215	0.1
C_{di} ($i = 1, \dots, 6$) (10^6 Ns/m)	2	0.1
ζ_i ($i = 1, \dots, 6$) (%)	0.05	0.1

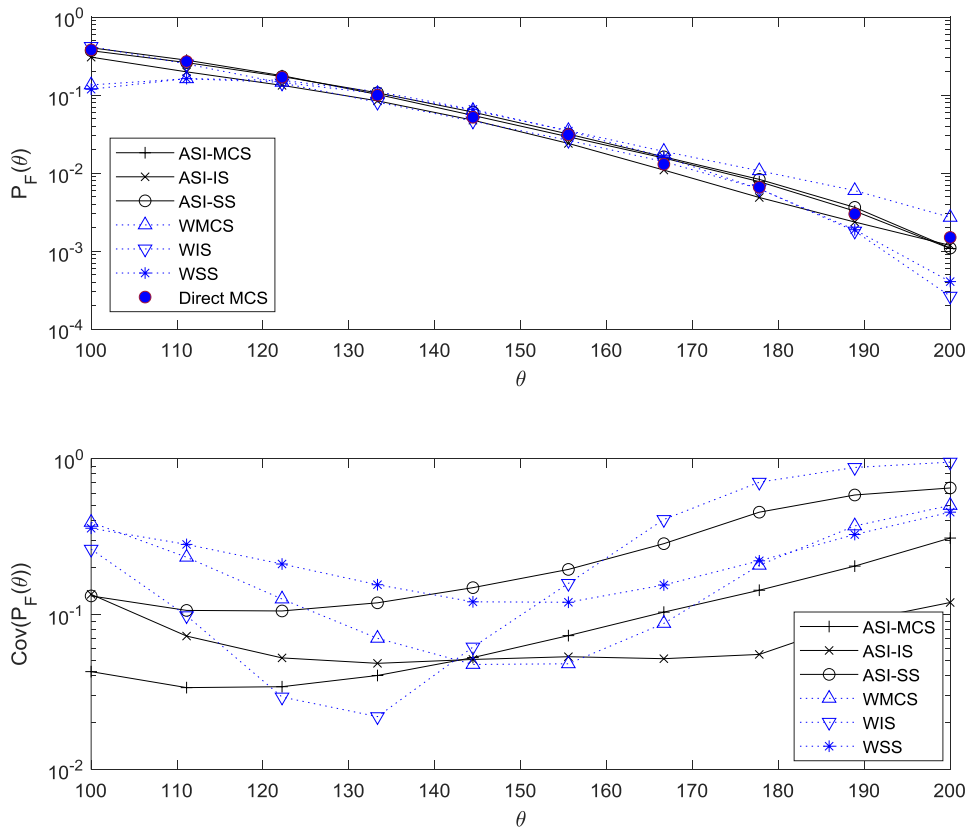
In the following, different approaches are applied to obtain the FPF of this frame structure with respect to θ . The proposed procedure with MCS, IS and SS is carried out in augmented space, i.e., ASI-MCS, ASI-IS and ASI-SS, respectively. And also, the weighted approach with MCS, IS, and SS is applied for comparison, i.e., WMCS, WIS, WSS. And it is assumed that the steel frame structure remains linear when the case for $b = 1.5\%$ is considered in this example.

486 **4.3.2 Results and discussion**

487 Table 6 lists the computational cost (number of the samples used) by each approach. For both
 488 the proposed ASI-procedure and weighted approach, their implementations involve the same
 489 number of samples, i.e., MCS comprises 10^4 samples, IS comprises 1000 samples, and SS comprises
 490 1000 for each level. These number of samples are selected as they provide a reasonable C.o.v. of
 491 FPF. Note that they are carried out in different spaces, i.e., the weighted approaches are carried
 492 out in the original random variable space whereas the proposed ASI procedure is implemented in
 493 the augmented space. Different number of failure samples are obtained. Note that for both ASI-IS
 494 and WIS, the importance sampling function is constructed based on the approach proposed in
 495 [33][35], and in this context, each of the generated sample will cause failure of system.

496 Fig. 8 shows the FPF results obtained by different methods. In addition, the direct MCS is
 497 carried out in ten independent simulation runs to generate point wise failure probability estimates,
 498 which are regarded as the exact reference results. Mostly, all the results by different approaches
 499 are consistent with the exact results. However, for this problem, the FPF results by the weighted
 500 approach possess remarkable error in both sides of the design domain i.e., when $\theta \in [100, 110]$
 501 and $\theta \in [190, 200]$. The reason is similar as that illustrated in Example 1: the weighted approach
 502 may just concentrate in an important failure region corresponding to $\theta = \theta_0$, while the proposed
 503 approach can explore all the important failure regions. At this point, the proposed ASI-approaches
 504 perform better than weighted approach in accuracy, as they produce more accurate results.

505



506

507

508

Fig. 8. The results of FPF obtained by the proposed approaches for Example 3

509

Table 6. Comparison of different methods for Example 3

Methods	No. of samples	No. of failure samples
ASI-MCS	10^4	927
ASI-IS	1000	1000
ASI-SS	1000×2	932
WMCS	10^4	442
WIS	1000	1000
WSS	1000×2	483
Direct MCS	$10^5 \times 10$	-

510

511 5. Conclusions

512 In this contribution, an efficient procedure has been presented for the estimation of the
 513 structural failure probability function (FPF). It utilizes the augmented idea to handle the problem,
 514 which transforms the FPF into an expression involving three terms. An algorithm is proposed to
 515 efficiently obtain the posterior distribution term, which is the key point of the estimation of the
 516 FPF. The proposed procedure comprises three different practical implementations to estimate the
 517 FPF, i.e., ASI-MCS, ASI-IS and ASI-SS.

518 Numerical examples have been presented to show the advantages of the proposed
 519 approaches. The following conclusions summarize the most salient features of the proposed.

520 (1) It demands a single reliability analysis in augmented space, and repeated evaluations of
 521 reliability are avoided.

522 (2) There is no need to estimate the posterior distribution by using density fitting methods. In
 523 fact, in the proposed procedure, this posterior distribution is expressed as an integral, which allows
 524 it to be estimated directly through the failure samples.

525 (3) There is no need to predict (or select beforehand) the shape of the posterior probability
 526 density function.

527 While the results presented are encouraging, it should be note that the proposed approach
 528 also possesses some limitations. Specifically, the number of the design parameters that can be
 529 handled effectively cannot be that large, e.g. not beyond 10. This is due to the fact that estimating
 530 probability densities (as required in the proposed approach) becomes challenging in high
 531 dimensions, as documented in [25] and [36].

532 Future research will involve application of the proposed procedure to other fields. For
 533 example, the proposed procedure can be easily applied for solving of reliability-based optimization
 534 problems combined with a decoupling strategy. Also, it can be used in reliability sensitivity analysis,
 535 which comprises the derivative of FPF and also in imprecise reliability problems [36], which involve
 536 the estimation of the extreme value of failure probability function over a certain region.

537

538 Declaration of competing interest

539 The authors declare that they have no known competing financial interests or personal
 540 relationships that could have appeared to influence the work reported in this paper.

541

542 Acknowledgments

543 The authors would like to acknowledge financial support from NSAF (Grant No. U1530122),
 544 the Aeronautical Science Foundation of China (Grant No. ASFC-20170968002), the Fundamental

545 Research Funds for the Central Universities of China (XMU-20720180072) and ANID (National
546 Agency for Research and Development, Chile) under its program FONDECYT, grant number
547 1180271.
548

549 Appendix A

550 This appendix further derives the expression for $\Delta(\mathbf{x}) = \int_{\theta}^{\bar{\theta}} f(\mathbf{x}|\theta) d\theta$. Note that since all
551 variables \mathbf{x} are assumed independent, calculating this integral is straightforward. For example, it
552 can be calculated using numerical algorithms. One alternative way is expressing $\Delta(\mathbf{x})$ as:

$$\Delta(\mathbf{x}) = \int_{\theta}^{\bar{\theta}} f(\mathbf{x}|\theta) d\theta = E_{\theta} \left[\frac{f(\mathbf{x}|\theta)}{\varphi(\theta)} \right] \quad (34)$$

553 where $E_{\theta}[\cdot]$ is the expectation under $\varphi(\theta)$. This means that it can be solved through sampling.

554 For the particular case where θ corresponds to the mean values of Gaussian random
555 variables, $\Delta(\mathbf{x})$ can be derived further. Suppose $x_i \sim N(\theta_i, \sigma_i^2)$, and $\theta_i \sim U[\underline{\theta}_i, \bar{\theta}_i]$ then $\Delta(\mathbf{x})$
556 can be obtained as:

$$\Delta(\mathbf{x}) = \prod_{i=1}^{n_{\theta}} \left[\Phi \left(\frac{\bar{\theta}_i - x_i}{\sigma_i} \right) - \Phi \left(\frac{\underline{\theta}_i - x_i}{\sigma_i} \right) \right] \quad (35)$$

557 where $\Phi(\cdot)$ is the cumulative probability function associated with a standard Gaussian
558 distribution.

559

560 Appendix B

561 This appendix derives the C.o.v. of the estimator $\hat{P}_F(\theta)$ in Eq. (27) calculated by the
562 proposed procedure with subset simulation.

563 In the following and for simplicity in notation, let $P_i = P(F_i|F_{i-1})$, $\hat{P}_i = \hat{P}(F_i|F_{i-1})$, $i =$
564 $1, \dots, m-1$, (where $F_0 = \Omega$), $P_m = P(F)$ and $I_{jk}^{(i)} = I_{F_i}(\mathbf{x}_{jk}^{(i-1)})$ where $\mathbf{x}_{jk}^{(i-1)}$ denotes the k -
565 th sample in the j -th Markov chain at simulation level i .

566 1) C.o.v. of \hat{P}_1

$$\delta_1 = Cov(\hat{P}_1) = \sqrt{\frac{1 - P_1}{P_1 N}} \approx \sqrt{\frac{1 - \hat{P}_1}{\hat{P}_1 N}} \quad (36)$$

567 2) C.o.v. of $\hat{P}_i (2 \leq i \leq m-1)$

568 At $(i-1)$ th level, suppose the number of Markov chain is N_C and N/N_C samples are
569 generated for each of these chains. It is assumed that the samples generated by different chains
570 are uncorrelated.

571 The variance of $\hat{P}_i (i = 2, \dots, m-1)$ is given by [11]:

$$\begin{aligned} Var(\hat{P}_i) &= E[\hat{P}_i - P_i]^2 = E \left[\frac{1}{N} \sum_{j=1}^{N_C} \sum_{k=1}^{N/N_C} (I_{jk}^{(i)} - P_i) \right]^2 \\ &= \frac{1}{N^2} \sum_{j=1}^{N_C} E \left[\sum_{1 \leftarrow k=1}^{N/N_C} (I_{jk}^{(i)} - P_i) \right]^2 \end{aligned} \quad (37)$$

572 For the j -th Markov chain

$$E \left[\sum_{1 \leftarrow 1}^{N/N_C} \left(I_{jk}^{(i)} - P_i \right) \right]^2 = \frac{N}{N_C} \left[R_i(0) + 2 \sum_{k=1}^{N/N_C-1} \left(1 - \frac{kN_C}{N} \right) R_i(k) \right] \quad (38)$$

573 Substituting Eq. (38) into (37) yields:

$$\text{Var}(\hat{P}_i) = \frac{R_i(0)}{N} \left[1 + 2 \sum_{k=1}^{N/N_C-1} \left(1 - \frac{kN_C}{N} \right) \frac{R_i(k)}{R_i(0)} \right] \quad (39)$$

574 Based on the Markov chain samples $\{(\mathbf{x}, \boldsymbol{\theta})_{jk}^{(i-1)}: j = 1, \dots, N_C; k = 1, \dots, N/N_C\}$ at the
575 $(i-1)$ th conditional level, the covariance $R_i(k) (k = 0, \dots, N/N_C - 1)$ can be estimated as:

$$\hat{R}_i(k) = \left(\frac{1}{N - kN_C} \sum_{j=1}^{N_C} \sum_{l=1}^{N/N_C-k} I_{jl}^{(i)} I_{j,l+k}^{(i)} \right) - \hat{P}_i^2 \quad (40)$$

576 3) C.o.v. of $\hat{P}_m(\boldsymbol{\theta})$

577 For the last level and for simplicity in notation, let $V_{jk}^{(m)} = \frac{I_F(\mathbf{x}^{(j)})f(\mathbf{x}^{(j)}|\boldsymbol{\theta})}{\Delta(\mathbf{x}^{(j)})}$ and $\hat{P}_m = \hat{P}_m(\boldsymbol{\theta})$.

578 Then the variance of \hat{P}_m is given by:

$$\begin{aligned} \text{Var}(\hat{P}_m) &= E[\hat{P}_m - P_m]^2 = E \left[\frac{1}{N} \sum_{j=1}^{N_C} \sum_{k=1}^{N/N_C} \left(V_{jk}^{(m)} - P_m \right) \right]^2 \\ &= \frac{1}{N^2} \sum_{j=1}^{N_C} E \left[\sum_{k=1}^{N/N_C} \left(V_{jk}^{(m)} - P_m \right) \right]^2 \end{aligned} \quad (41)$$

579 For the j -th Markov chain,

$$E \left[\sum_{k=1}^{N/N_C} \left(V_{jk}^{(m)} - P_m \right) \right]^2 = \frac{N}{N_C} \left[R_m(0) + 2 \sum_{k=1}^{N/N_C-1} \left(1 - \frac{kN_C}{N} \right) R_m(k) \right] \quad (42)$$

580 Substituting Eq. (42) into (41) yields:

$$\text{Var}(\hat{P}_m) = \frac{R_m(0)}{N} \left[1 + 2 \sum_{k=1}^{N/N_C-1} \left(1 - \frac{kN_C}{N} \right) \frac{R_m(k)}{R_m(0)} \right] \quad (43)$$

581 Based on the Markov chain samples $\{(\mathbf{x}, \boldsymbol{\theta})_{jk}^{(m-1)}: j = 1, \dots, N_C; k = 1, \dots, N/N_C\}$ at the
582 $(m-1)$ th conditional level, the covariance $R_m(k) (k = 0, \dots, N/N_C - 1)$ is estimated as:

$$R_m(k) \approx \hat{R}_m(k) = \left(\frac{1}{N - kN_C} \sum_{j=1}^{N_C} \sum_{l=1}^{N/N_C-k} V_{jl}^{(m)} V_{j,l+k}^{(m)} \right) - \hat{P}_m^2 \quad (44)$$

583 4) C.o.v. of $\hat{P}_F(\boldsymbol{\theta})$

584 At last, suppose all \hat{P}_i ($i = 1, \dots, m$) are uncorrelated [11], then the C.o.v. of $\hat{P}_F(\boldsymbol{\theta})$ is given
585 by:

$$\text{Cov}[\hat{P}_F(\boldsymbol{\theta})] = \sqrt{\sum_{i=1}^m \delta_i^2} = \sqrt{\sum_{i=1}^m \frac{\text{Var}(\hat{P}_i)}{P_i^2}} \approx \sqrt{\sum_{i=1}^m \frac{\text{Var}(\hat{P}_i)}{\hat{P}_i^2}} \quad (45)$$

586 where $\text{Var}(\hat{P}_i)$ can be calculated according to Eqs. (36), (39) and (43).

587

588 **References**

- 589 [1] Enevoldsen I, Sørensen JD. Reliability-based optimization in structural engineering. *Structural*
590 *Safety* 1994; 15(3):169-96.
- 591 [2] Valdebenito MA, Schuëller GI. A survey on approaches for reliability-based optimization.
592 *Structural and Multidisciplinary Optimization* 2010; 42(5):645-663.
- 593 [3] Valdebenito MA, Jensen HA, Hernandez HB, Mehrez L. Sensitivity estimation of failure
594 probability applying line sampling. *Reliability Engineering and System Safety* 2018; 171:99-
595 111.
- 596 [4] Papaioannou I, Breitung K, Straub D. Reliability sensitivity estimation with sequential
597 importance sampling. *Structural Safety* 2018; 75: 24-34
- 598 [5] Zou T, Mahadevan S. A direct decoupling approach for efficient reliability-based design
599 optimization. *Structural and Multidisciplinary Optimization* 2006; 31(3):190-200.
- 600 [6] Yuan XK, Lu ZZ. Efficient approach for reliability-based optimization based on weighted
601 importance sampling approach. *Reliability Engineering and System Safety* 2014; 132: 107-114.
- 602 [7] Rackwitz R, Fiessler B. Structural reliability under combined random load sequences. *Comput.*
603 *Struct* 1978; 9 (5):489–494.
- 604 [8] Breitung K. Asymptotic approximations for probability integrals. *Probabilistic Engineering*
605 *Mechanics* 1989; 4 (4): 187–190.
- 606 [9] Metropolis N, Ulam S. The Monte Carlo method. *J Am Stat Assoc* 1949; 44(247):335–41.
- 607 [10] R.E. Melchers. Importance sampling in structural systems. *Struct Safety* 1989; 6(1):3–10.
- 608 [11] Au SK, Beck JL. Estimation of small failure probabilities in high dimensions by subset simulation.
609 *Probabilistic Engineering Mechanics* 2001; 16(4): 263–77.
- 610 [12] Koutsourelakis PS, Pradlwarter HJ, Schuëller GI. Reliability of structures in high dimensions,
611 Part I: algorithms and application. *Probabilistic Engineering Mechanics* 2004; 19: 409-417.
- 612 [13] Gasser M, Schuëller GI. Reliability-based optimization of structural systems. *Mathematical*
613 *Methods of Operations Research* 1997; 46(3):287-307.
- 614 [14] Jensen HA. Structural optimization of linear dynamical systems under stochastic excitation: A
615 moving reliability database approach. *Computer Methods in Applied Mechanics and*
616 *Engineering* 2005; 194(12-16):1757-78.
- 617 [15] Sacks J, Welch WJ, Mitchell TJ, Wynn HP. Design and analysis of computer experiments. *Stat*
618 *Sci* 1989; 4:409–423.
- 619 [16] Jones DR, Schonlau M, Welch WJ Efficient global optimization of expensive black-box functions.
620 *J Glob Optim* 1998, 13(4):455–492.
- 621 [17] Cortes C, Vapnik VN. Support vector networks. *Machine Learning*, 1995, 20(3):273–297.
- 622 [18] Vapnik VN. An overview of statistical learning theory. *IEEE Transaction on Neural Networks*
623 1999, 10(5):988–998.
- 624 [19] Echard B., Gayton N., Lemaire M. AK-MCS: an active learning reliability method combining
625 Kriging and Monte Carlo Simulation. *Struct. Saf.* 2011, 33:145-154.
- 626 [20] Li HS, Lu ZZ, Yue ZF. Support vector machine for structural reliability analysis. *Applied*
627 *Mathematics and Mechanics* 2006, 27 (10):1295-1303.
- 628 [21] Wei PF, Song JW, Bi SF, Broggi M, Beer M. Non-intrusive stochastic analysis with parameterized
629 imprecise probability models: I. performance estimation, *Mech. Syst. Signal Process* 2019,
630 124:349–368.

- 631 [22] Wei PF, Song JW, Bi SF, Broggi M, Beer M. Non-intrusive stochastic analysis with parameterized
632 imprecise probability models: II. Reliability and rare events analysis, *Mech. Syst. Signal Process*
633 2019, 126:227–247.
- 634 [23] Yuan XK. Local estimation of failure probability function by weighted approach, *Probabilistic*
635 *Engineering Mechanics* 2013; 34: 1-11.
- 636 [24] Yuan XK, Zheng ZX, Zhang BQ. Augmented line sampling for approximation of failure
637 probability function in reliability-based analysis. *Applied Mathematical Modelling* 2020, 80:
638 895-910.
- 639 [25] Au SK. Reliability-based design sensitivity by efficient simulation. *Computers and Structures*
640 2005; 83(14):1048-61.
- 641 [26] Ching J, Hsieh YH. Local estimation of failure probability function and its confidence interval
642 with maximum entropy principle. *Probabilistic Engineering Mechanics* 2007; 22(1):39-49.
- 643 [27] Ching J, Hsieh YH. Approximate reliability-based optimization using a three-step approach
644 based on subset simulation. *Journal of Engineering Mechanics-ASCE* 2007; 133(4):481-493.
- 645 [28] Casella G, Berger R.L. *Statistical Inference*, 2nd edn(M). Duxbury Press, 2001.
- 646 [29] Au SK, Beck JL. A new adaptive importance sampling scheme for reliability calculations.
647 *Structural Safety* 1999, 21(2):135-158.
- 648 [30] Au SK, Beck JL, Zuev KM, Katafygiotis LS. Discussion of paper by F. Miao and M. Ghosn
649 “Modified subset simulation method for reliability analysis of structural systems”, *Structural*
650 *Safety*, 33:251–260, 2011. *Structural Safety* 2011; 34:379-380.
- 651 [31] Cai ZY. Precision design of roll-forging die and its application in the forming of automobile
652 front axles. *Journal of Materials Processing Technology* 2005, 168(1):95-101.
- 653 [32] Xiao SN, Lu ZZ. Structural Reliability Analysis Using Combined Space Partition Technique and
654 Unscented Transformation. *Journal of Structural Engineering* 2016, 142(11):04016089.
- 655 [33] Au SK, Beck JL. First excursion probabilities for linear systems by very efficient importance
656 sampling. *Probabilistic Engineering Mechanics* 2001, 16 (3):193-207.
- 657 [34] Valdebenito, M.; Misraji, M.; Jensen, H. & Mayorga, C. Sensitivity Estimation of First Excursion
658 Probabilities of Linear Structures Subject to Stochastic Gaussian Loading. *Computers &*
659 *Structures*, 2021, 248: 106482.
- 660 [35] Yuan XK, Gu J, Wu MY, Zhang F. Efficient reliability-based optimization of linear dynamic system
661 with random structural parameters, preprint submitted to elsevier (2020).
- 662 [36] Yuan XK, Faes MGR, Liu SL, Valdebenito MA, Beer M. Efficient imprecise reliability analysis
663 using the Augmented Space Integral, *Reliability Engineering & System Safety* 2021, 210:
664 107477.